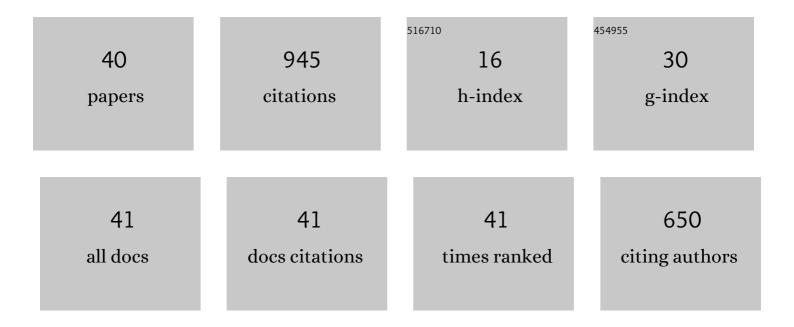
Mario J Kriegel

List of Publications by Year in descending order

Source: https://exaly.com/author-pdf/2086910/publications.pdf Version: 2024-02-01



MADIO I KDIECEL

#	Article	IF	CITATIONS
1	The αâ†'ï‰ and βâ†'ï‰ phase transformations in Ti–Fe alloys under high-pressure torsion. Acta Materialia, 20 337-351.	18, 144, 7.9	118
2	Phase Transformations in Ti–Fe Alloys Induced by Highâ€Pressure Torsion. Advanced Engineering Materials, 2015, 17, 1835-1841.	3.5	95
3	Promoting abnormal grain growth in Fe-based shape memory alloys through compositional adjustments. Nature Communications, 2019, 10, 2337.	12.8	79
4	Formation of the ω Phase in the Titanium—Iron System under Shear Deformation. JETP Letters, 2020, 111, 568-574.	1.4	65
5	Phase transformations in the severely plastically deformed Zr–Nb alloys. Materials Letters, 2012, 81, 225-228.	2.6	61
6	Cyclic degradation in bamboo-like Fe–Mn–Al–Ni shape memory alloys — The role of grain orientation. Scripta Materialia, 2016, 114, 156-160.	5.2	61
7	Transformations of α' martensite in Ti–Fe alloys under high pressure torsion. Scripta Materialia, 2017, 136, 46-49.	5.2	44
8	Thermodynamic assessment of the Cr–Ti and first assessment of the Al–Cr–Ti systems. Intermetallics, 2011, 19, 1222-1235.	3.9	32
9	Calorimetric investigation of the La2Zr2O7, Nd2Zr2O7, Sm2Zr2O7 and LaYO3 compounds and CALPHAD assessment of the La2O3–Y2O3 system. Thermochimica Acta, 2011, 526, 50-57.	2.7	30
10	On the microstructural and functional stability of Fe-Mn-Al-Ni at ambient and elevated temperatures. Scripta Materialia, 2019, 162, 442-446.	5.2	27
11	Transformation Pathway upon Heating of Ti–Fe Alloys Deformed by Highâ€Pressure Torsion. Advanced Engineering Materials, 2018, 20, 1700933.	3.5	23
12	Heat capacity for the Eu2Zr2O7 and phase relations in the ZrO2–Eu2O3 system: Experimental studies and calculations. Thermochimica Acta, 2013, 558, 74-82.	2.7	22
13	Cyclic Degradation Behavior of \$\$ langle 001 angle \$\$ âŸ 001 ⟩ -Oriented Fe–Mn–Al–Ni Single Crystals in Tension. Shape Memory and Superelasticity, 2017, 3, 335-346.	2.2	22
14	Effective Temperature of High Pressure Torsion in Zr-Nb Alloys. High Temperature Materials and Processes, 2012, 31, .	1.4	20
15	Thermophysical properties of pyrochlore and fluorite phases in the Ln2Zr2O7–Y2O3 systems (Ln=La,) Tj ETQq1 Compounds, 2014, 586, 118-128.	1 0.7843 5.5	14 rgBT /Ov 19
16	Thermodynamic assessment and experimental investigation of the systems Al–Fe–Mn and Al–Fe–Mn–I Calphad: Computer Coupling of Phase Diagrams and Thermochemistry, 2019, 66, 101621.	^{Vi} 1.6	19
17	Effect of Melt Conditioning on Removal of Fe from Secondary Al-Si Alloys Containing Mg, Mn, and Cr. Metallurgical and Materials Transactions A: Physical Metallurgy and Materials Science, 2018, 49, 6375-6389.	2.2	15
18	Thermodynamic and physical properties of Zr3Fe and ZrFe2 intermetallic compounds. Intermetallics, 2019, 109, 189-196.	3.9	14

MARIO J KRIEGEL

#	Article	IF	CITATIONS
19	Thermal Stability of Athermal ωâ€Ti(Fe) Produced upon Quenching of βâ€Ti(Fe). Advanced Engineering Materials, 2019, 21, 1800158.	3.5	14
20	Thermodynamics of martensite formation in Fe–Mn–Al–Ni shape memory alloys. Scripta Materialia, 2021, 192, 26-31.	5.2	14
21	High-temperature phase equilibria with the bcc-type β (AlMo) phase in the binary Al–Mo system. Intermetallics, 2017, 83, 29-37.	3.9	12
22	Formation and Thermal Stability of ω-Ti(Fe) in α-Phase-Based Ti(Fe) Alloys. Metals, 2020, 10, 402.	2.3	12
23	Thermophysical properties of pyrochlore and fluorite phases in the Ln2Zr2O7–Y2O3 systems (Ln = La,) Tj ETÇ Sm2Zr2O7–Y2O3. Journal of Alloys and Compounds, 2015, 625, 200-207.	9q1 1 0.78 5.5	4314 rgBT /O 10
24	Thermodynamic assessment and experimental investigation of the Al–Mn–Ni system. Calphad: Computer Coupling of Phase Diagrams and Thermochemistry, 2019, 64, 78-89.	1.6	10
25	Functionally graded structures realized based on Fe–Mn–Al–Ni shape memory alloys. Scripta Materialia, 2021, 194, 113619. In situ characterization of the functional degradation of a ≺mml:math	5.2	10
26	xmlns:mml="http://www.w3.org/1998/Math/MathML" altimg="si1.svg"> <mml:mrow><mml:mo>[</mml:mo><mml:mrow><mml:mn>00</mml:mn><mml:mover accent="true"><mml:mn>1</mml:mn><mml:mo>Â⁻</mml:mo></mml:mover </mml:mrow><mml:mo>]orientated Fe–Mn–Al–Ni single crystal under compression using acoustic emission measurements.</mml:mo></mml:mrow>	no>∕/mml	:mrow>
27	Acta Materialia 2021, 220, 117333 New experimental investigations of phase relations in the Yb2O3–Al2O3 and ZrO2–Yb2O3–Al2O3 systems and assessment of thermodynamic parameters. Journal of the European Ceramic Society, 2015, 35, 2855-2871.	5.7	9
28	Experimental Investigations of the Fe-Mn-Ti System in the Concentration Range of up to 30Âat.% Ti. Journal of Phase Equilibria and Diffusion, 2020, 41, 457-467.	1.4	9
29	Phase equilibria at 1473K in the ternary Al–Cr–Ti system. Journal of Alloys and Compounds, 2013, 550, 519-525.	5.5	8
30	Nanoscale twinning in Fe–Mn–Al–Ni martensite: a backscatter Kikuchi diffraction study. Journal of Applied Crystallography, 2021, 54, 54-61.	4.5	8
31	The ternary Al–Mo–Ti system revisited: Phase equilibria of Al63(Mo,Ti)37. Journal of Alloys and Compounds, 2019, 811, 152055.	5.5	7
32	An orthorhombic D022-like precursor to Al8Mo3 in the Al–Mo–Ti system. Journal of Alloys and Compounds, 2020, 823, 153807.	5.5	7
33	High temperature phase equilibria in the Ti-poor part of the Al–Mo–Ti system. Journal of Alloys and Compounds, 2017, 706, 616-628.	5.5	6
34	Binary Ti–Fe system. Part I: Experimental investigation at high pressure. Calphad: Computer Coupling of Phase Diagrams and Thermochemistry, 2021, 74, 102322.	1.6	6
35	Constitution of the liquidus and solidus surfaces of the Al–Ti–Cr system. Journal of Alloys and Compounds, 2014, 584, 438-446.	5.5	5
36	Nanoscale twinning and superstructures of martensite in the Fe–Mn–Al–Ni system. Materialia, 2021, 16, 101062.	2.7	5

MARIO J KRIEGEL

#	Article	IF	CITATIONS
37	Binary Ti–Fe system. Part II: Modelling of pressure-dependent phase stabilities. Calphad: Computer Coupling of Phase Diagrams and Thermochemistry, 2022, 76, 102383.	1.6	5
38	Specific Heat Capacity Measurements of Intermetallic Phases in the Ternary Al-Ti-Cr System. Journal of Phase Equilibria and Diffusion, 2014, 35, 658-665.	1.4	4
39	Experimental investigation of phase relations and thermodynamic properties in the system ZrO 2 –Eu 2 O 3 –Al 2 O 3. Journal of the European Ceramic Society, 2016, 36, 1455-1468.	5.7	4
40	Thermodynamic re-modelling of the Cu–Nb–Sn system: Integrating the nausite phase. Calphad: Computer Coupling of Phase Diagrams and Thermochemistry, 2022, 77, 102409.	1.6	4